



EUROfusion

WPPMI-CPR(18) 20643

Yu. Igitkhanov et al.

Vapor Shielding Effect on the DEMO Tungsten Divertor Plate

Preprint of Paper to be submitted for publication in Proceeding of
The Technology of Fusion Energy (TOFE 2018)



This work has been carried out within the framework of the EUROfusion Consortium and has received funding from the Euratom research and training programme 2014-2018 under grant agreement No 633053. The views and opinions expressed herein do not necessarily reflect those of the European Commission.

This document is intended for publication in the open literature. It is made available on the clear understanding that it may not be further circulated and extracts or references may not be published prior to publication of the original when applicable, or without the consent of the Publications Officer, EUROfusion Programme Management Unit, Culham Science Centre, Abingdon, Oxon, OX14 3DB, UK or e-mail Publications.Officer@euro-fusion.org

Enquiries about Copyright and reproduction should be addressed to the Publications Officer, EUROfusion Programme Management Unit, Culham Science Centre, Abingdon, Oxon, OX14 3DB, UK or e-mail Publications.Officer@euro-fusion.org

The contents of this preprint and all other EUROfusion Preprints, Reports and Conference Papers are available to view online free at <http://www.euro-fusionscipub.org>. This site has full search facilities and e-mail alert options. In the JET specific papers the diagrams contained within the PDFs on this site are hyperlinked

VAPOR SHIELDING EFFECT ON DEMO DIVERTOR LIFETIME

Yuri Igitkhanov*, Boris Bazylev*¹ and Lorenzo Boccaccini*

*Karlsruhe Institute of Technology

¹South Ural State University, 454080 Chelyabinsk, Lenin Prospect 76, Russian Federation
juri.igitkhanov@partner.kit.edu; boris.bazylev@partner.kit.edu; lorenzo.boccaccini@kit.edu

ABSTRACT

The impact of the edge-localized modes on the tungsten divertor erosion by taking into account the screening effect of vapor shielding is analyzed for DEMO steady state operation condition. The evaluation of tungsten ablation, energy radiation and absorption by divertor plate due to a single ELM impact is calculated by using a model of vapor shielding inserted in the MEMOS code. The effect of repetitive ELM impact and the tungsten melt layer formation is described by using the model of W monoblock with a compliance layer of Cu alloy between W and EUROFER water cooling tube.

It is shown that the vapor plasma shielding results in saturation of the single ELM energy accumulated by the divertor plate at the level of about $\sim 0.5 \text{ MJ/m}^2$ and the ablation thickness can reach about $0.01 \text{ }\mu\text{m}$. The total number of ablated particles is rather critical for the shielding formation and the life-time of the divertor plate depends strongly on this effect.

KEYWORDS

Vapor shielding, DEMO divertor, Edge localized mode, Erosion of divertor plates, Tungsten melting.

1. INTRODUCTION

In the DEMO fusion reactor the conventional H-mode operation regime with Edge Localized Modes (ELMs) will cause the divertor material distraction and the necessity of the often replacement of the divertor modules [1]. The ELM power impact will melt the tungsten armor and the evaporated material will radiate the heating power thus lowering the energy absorbed by divertor plates. The evaluation of tungsten ablation, energy radiation and absorption by divertor plate due to a single and multiple ELMs impact on divertor plates is calculated by using a model of vapor shielding inserted in the MEMOS code [2].

The expected ELMs signatures in DEMO are estimated by extrapolating predictions found for ITER and by using the scaling arguments made from existing experiments [3- 6]. Type I ELMs size (engineering load) can be estimated in the range of $3\text{-}10 \text{ MJ/m}^2$ with the timescale for the rise and decay phase of the ELM power deposition at the divertor target in the range $\tau \sim 3\text{-}1 \text{ ms}$, correspondingly. The frequency of unmitigated ELM is expected $\leq 1 \text{ Hz}$ [3]. The experimental time dependence of the ELM power deposition $P(t)$ per m^2 is reproduced satisfactorily by the model [7]:

$$P(t) \simeq \left(1 + (\tau/t)^2\right) \cdot (\tau/t)^2 \cdot \exp\left(-(\tau/t)^2\right) \quad (1)$$

Apart of it we also use a rectangular and triangular model for power evolution. The power flux to the divertor during the ELM has a maximum near the separatrix, with a similar decay length at the divertor target to that measured between ELMs and is toroidally symmetric independent from distance from the separatrix. The power fluxes in the far SOL are typically more than one order of magnitude lower than for the near SOL. A Gaussian shape of the ELM pulse radial distribution with a full width at half maximum $\sim 3 \text{ cm}$ is used.

In the present work, the 2015 DEMO design of ~2GW of fusion power with the major radius $R=8.8\text{m}$, the aspect ratio $A=3$, the toroidal magnetic field $B=6\text{T}$ and the safety factor $q_a=3$ is considered [8]. A design concept of mono-block type water cooled DEMO divertor module with Cu alloy OFHC (Oxygen Free High Conductivity) /EUROFER tube [9,4] have been employed here for steady state operation with the repetitive ELMs.

For DEMO, where several tens of dpa are expected on the PFCs, the selection and qualification of suitable materials is an issue. At present, W alloys (W-2%Re) are the primary refractory materials for the PFC in DEMO and is considered as an efficient heat diffuser due to a high thermal conductivity. However, W features a very narrow operational temperature window which limited by the ductile–brittle transition temperature (DBTT) from below and by recrystallization and creep strength from above.

In our study we assumed that the maximum W temperature must be between 500°C and 1300°C . The oxide dispersion strengthened (ODS) stainless steel EUROFER ODS (9%Cr) is chosen as structural material with the high temperature creep resistance. With regard to EUROFER, the minimum allowable temperature boundary is limited by high DBTT variation under irradiation ($\geq 300\text{-}350^\circ\text{C}$). The upper temperature boundary is suggested as $\sim 550^\circ\text{C}$ and is limited by creep strength.

The upper allowable temperature boundary for OFHC Cu is limited by the low thermal creep at temperatures above $\sim 0.5T_m$, where $T_m \sim 1356\text{ K}$ is the melting point. Since the pipe is reinforced by the EUROFER inner tube, the Cu allow could sustain a slightly higher temperature. We suggest the operation window within 300°C and 650°C [9, 10]. Since there is no reliable data of thermo-mechanical properties under irradiation above 5dpa, we, follow [9], assume 20% of degradation of thermal conductivity in Cu OFHC and 10% in EUROFER and W, which corresponds to $\sim 5\text{dpa}$. Below we assume that the maximal values of material temperatures must be within these windows.

The heat flux profiles of Type I ELMs in experiments show a clear peak near the separatrix strike point (SSP) with random spatial variations of SSP position and of heat flux for sequential ELMs [10]. It seems justified to assume that the position of SSP at the divertor plate stochastically moves obeying the Gaussian distribution, with some dispersion. In this paper we ignore this movement.

In the paper we mainly consider first the effect of single and then the multiple ELM incident energy reduction due to the formation of the tungsten vapor shielding on DEMO divertor armor.

2. EFFECT OF SINGL ELM IMPAKT

First, the impact of a single ELM is considered. In the time scale of 1-3ms the power flux heats only the tungsten thin surface, bounded with plasma. Calculations show that the shielding effect as a response of tungsten material on the incident plasma heat flux results in saturation of the absorbed energy accumulated by the divertor plate at some level which depends on the pulse duration and the pulse shape (see Fig. 1).

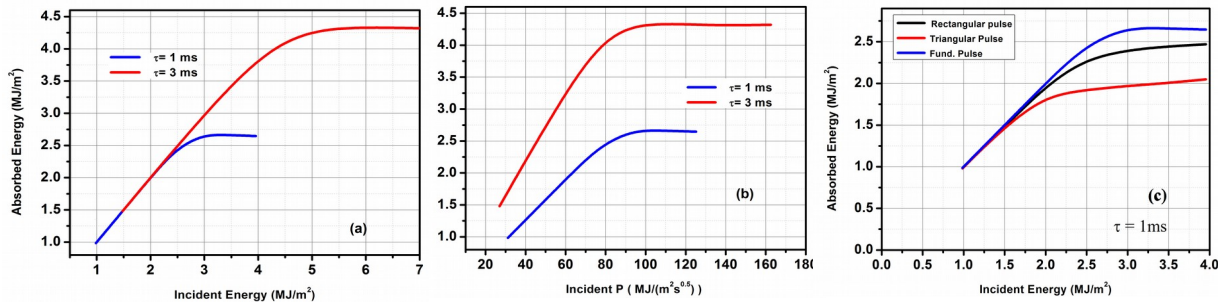


Figure 1 The dependence of absorbed energy by evaporated tungsten vs the ELM incident energy per unit area on the divertor plate for ELMs time duration τ of 1ms and 3ms (a), the same for incident energy normalised to the sqrt (sec) (b) and the absorbed energy for the different shape of the ELM pulses and time duration $\tau=1$ ms (c).

Dependence of the saturated absorbed energy on the pulse duration behaves proportional to the squared root of the pulse duration as it is shown in the Fig. 2.

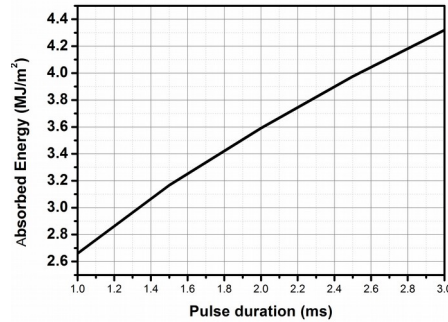


Figure 2 Saturated value of the absorbed energy as a function of the pulse durations in ms; a rectangular pulse shape.

The evolution of tungsten armour temperature and for 1 and 3ms for rectangular ELM pulse shape and corresponding vapour flux is shown in Fig.3(a,b).

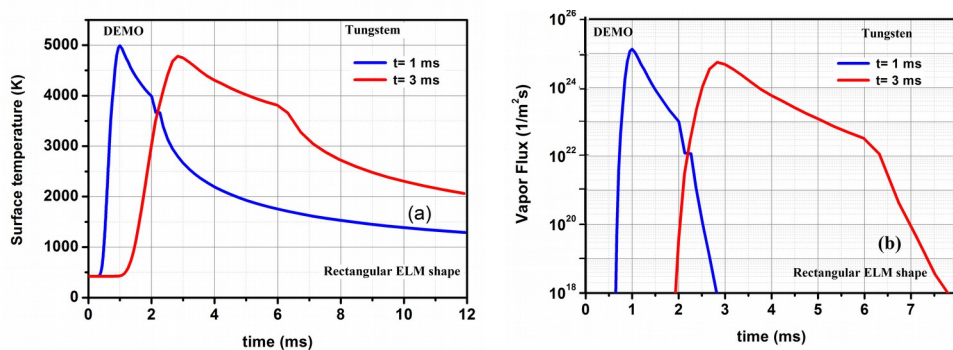


Figure 3 The evolution of tungsten armour temperature for 1 and 3ms for rectangular ELM pulse shape (a) and corresponding vapour flux (b); a rectangular pulse shape.

3. EFFECT OF MULTIPLE ELM IMPAKT

In the DEMO stationary operation the unmitigated repetitive ELMs are expected to occur at a frequency of about ~ 1 Hz [3]. The evolution of the tungsten temperature and the tungsten vapour flux are shown in Fig. 4 and Fig.5. For repetitive ELMs impact the water cooling conditions of divertor plates are taken into account since the heating time becomes comparable with the thermal conductivity time of materials. Calculations use the power water reactor (PWR) cooling conditions with water temperature in tube inlet $T_b = 325$ °C, inlet pressure $P = 15.5$ MPa, and velocity $v = 20$ m/s.

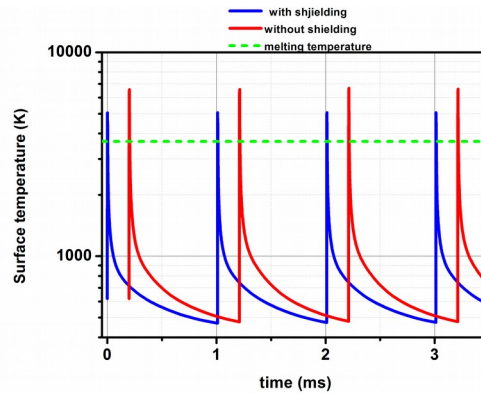


Figure 4 Evolution of the tungsten surface temperature during the ELMs under the PWR cooling conditions. To distinguish the cases with and without shielding they are shifted in time axes. The dashed line marks the melting temperature.

Calculations show that a difference in the maximum temperature due to vapour screening is about 1500K (see Fig. 4). However, the screening effect does not prevent the W armor surface melting during the ELMs spikes. The average molten layer is about 200 μ m without screening and drops down to 80 μ m when vapor screening is taken into account. Between ELMs the surface temperature cools rapidly and the molten layer solidifies. The tungsten vapour fluxes during four pulses is shown in Fig. 5

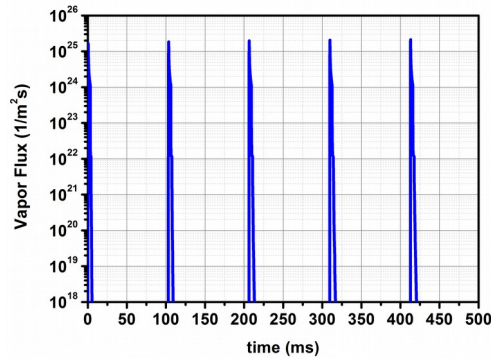


Figure 5 Evolution of the vapor flux caused by the ELMs impact.

The temperatures of Cu OFHC and Eurofer, on the other hand, stay within the allowable temperature range at all times, thus providing mechanical stability of the divertor module. This is achieved by the higher water coolant temperature and higher pressure as compared to ITER-like cooling conditions [4]. Although Eurofer and Cu OFHC temperatures stay in a tolerable range for ELMy DEMO heat loads when PWR cooling conditions are applied, the melting and erosion of W during ELM impact considerably limits the life time of the divertor module. The W surface melts during ELMs, but cools rapidly and solidifies after each ELM impact.

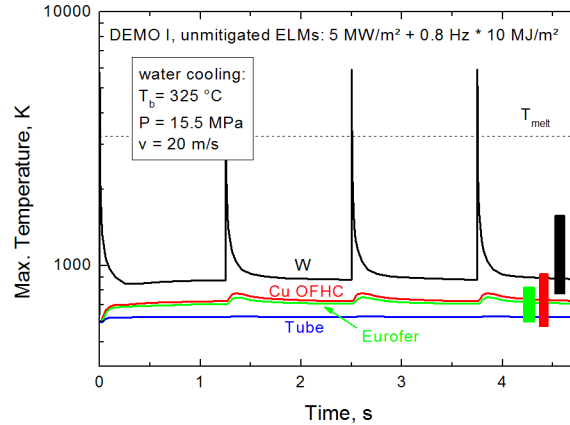


Figure 6. Evolution of the maximum temperature for W armor, EUROFER diffuser, copper alloy and stainless steel tube. DEMO operation with unmitigated ELMs and PWR cooling. The bars on the right mark the allowable temperature range of the respective materials.

Although Eurofer and Cu OFHC temperatures stay in a tolerable range for ELM DEMO heat loads when PWR cooling conditions are applied, the melting and erosion of W during ELM impact considerably limits the life time of the divertor module.

3. CONCLUSIONS

We calculate here the impact of shielding effects as a response of the divertor plate material (Tungsten) on the incident plasma heat flux caused by Type I ELM envisage in DEMO reactor. The vapor plasma shielding results in the saturation of the energy (per unit surface area) accumulated by the plate at some level which can be significantly lower than the energy delivered by the single and the multiple ELMs. The previous simulation in [11] show that for the repetitive multiple ELMs with $W_{ELM} \sim 1-10 \text{ MJ/m}^2$ the pressure gradient of the plasma shield is mainly responsible for an intensive melt motion of tungsten target with the melt velocities of 0.5 m/s and the surface roughness of 0.1 μm . Due to the small melt velocity and the small re-solidification time of few ms the melt splashing does not develop therefore all mass losses are due to target evaporation.

For many ELMs, at fixed separatrix strike point position the maximum crater depth exceeds the evaporation thickness. Assumption on stochastic motion of separatrix strike point along the target surface could probably decreases the total erosion [11].

The melting and erosion of W during ELM impact considerably limits the lifetime of the divertor module. Without screening the molten layer is estimated as 200 μm , whereas the screening lowers this value down to 80 μm .

Although Eurofer and Cu OFHC temperatures stay in a tolerable range for ELM DEMO heat loads when PWR cooling conditions are applied, the melting and erosion of W during ELM impact considerably limits the lifetime of the divertor module even under vapor shielding power mitigation.

ACKNOWLEDGMENTS

This work has been carried out within the framework of the EUROfusion Consortium and has received funding from the Euratom research and training programme 2014-2018 under grant agreement No 633053. The views and opinions expressed herein do not necessarily reflect those of the European Commission.

REFERENCES

1. R. Pitts, Physics specification of heat loads to tokamak reactor PFCs: a case study from ITER, invited talk , ISFRNT-13, Kyoto, 2017
2. B. Bazylev et al., Physica Scripta 2011, volT145 p .014054
3. Yu. Igitkhanov, B. Bazylev, IEEE Transaction on Plasma Science, 42 (2014) 2284-2290.
4. R. Fetzer, Yu. Igitkhanov, B. Bazylev, Fusion Engineering and Design, 98–99, 2015, pp. 1290-1293
5. T. Eich, B. Sieglin, A.J. Thornton et al., ELM divertor peak energy fluence scaling to ITER with data from JET, MAST and ASDEX upgrade, Nuclear Materials and Energy 12 (2017) 84–90;
6. A. Loarte, G. Saibene, R. Sartori et. al., Characteristics of Type I ELM Energy and Particle Losses in Existing Devices and their Extrapolation to ITER, preprint EFDA–JET–PR(03)32
7. Fundamenski,W.,et al., Plas.Phys.Cont.Fus. 48 (2006) 109
8. R. Wenninger et al., Nucl. Fus., vol. 57, pp. 016011, 2017.
9. A. Li-Puma, , M. Richou, P. Magaud, et. al., Fusion Engineering and Design 88 (2013) 1836-1843.
10. S.Zinkle, N.Ghoniem, Fus.Eng. and Des.,51-52, 2000, 55
11. Yu. Igitkhanov,B. Bazylev, S. Pestchanyi and L. Boccaccini, Plasma facing materials lifetime in fusion reactor, 27th Symp.on Fusion Tech. (SOFT 2012), Liege, B, September 24-28, 2012.